Int. J. Heat Mass Transfer. Vol. 35, No. 1, pp. 29–42, 1992
Printed in Great Britain

0017–9310/92 $5.00 + 0.00

An effective installation of turbulence promoters for heat transfer augmentation in a vertical rib-heated channel

Y. H. HUNG† and H. H. LIN
Department of Power Mechanical Engineering, National Tsing Hua University, Hsinchu, Taiwan 30043, R.O.C.

(*Received* 4 *January* 1991 *and in final form* 15 *March* 1991)

Abstract—Parameter studies including the channel spacing, convective heat flux, channel inlet velocity, turbulence-promoter location and height on heat transfer performance and pressure drop in a vertical rib-heated channel have been explored in detail. In addition, the rib/overall channel Nusselt numbers and the coefficient of channel pressure drop C_p are correlated and presented in terms of relevant dimensionless parameters studied. The experimental results show that the installation of turbulence promoter on the opposite shrouding insulated wall in the vertical rib-heated channel can effectively enhance all the rib heat transfer performances in the channel and avoid hot spots occurring in the 'quasi-equilibrium' high-temperature regime. Taking both thermal and flow aspects into consideration simultaneously, Nu and C_p increase hand in hand with increasing ratio of promoter height to channel spacing t/H. This tendency is consistent with the increased levels of flow disturbance, or turbulence mixing, promoted by the protruding ribs and the installed turbulence promoter.

INTRODUCTION

IN MANY electronic packages, the heat dissipating components are usually mounted on vertical parallel printed circuit boards (PCBs), which form an array of vertical channels. Thus, a vertical two-dimensional plate with or without a shrouding wall is a frequently encountered configuration in convective air cooling of electronic equipment. Generally, packaging constraints and electronic considerations, as well as devices or system operating modes, lead to a wide variety of heat dissipation profiles along the channel walls. In many cases of interest, four kinds of thermal wall conditions were proposed to yield approximate conditions in the prediction of the thermal performance of such configurations, that, is, two symmetric isothermal plates; a single isothermal plate and an insulated plate; two symmetric isoflux plates; and, a single isoflux plate and an insulated plate [1].

As we know, identical flat pack electronic components mounted on a PCB are often placed next to one another. When each component dissipates approximately the same amount of power, the heat load will approach a uniform isoflux heat profile. Taking any row of electronic components into consideration, the heat dissipation can be evaluated as a uniformly distributed isoflux heating, and this row of electronic components can be properly simulated by a two-dimensional large rib with isoflux heating. Therefore, compared with a smooth isoflux heating plate or a plate mounted with horizontally parallel ribs under isothermal heating, an insulated plate mounted with an array of horizontally parallel ribs under isoflux heating is more appropriate to represent the real geometric configuration and heating condition of the vertical PCB array.

To explore the forced-convection heat transfer characteristics in such a vertical rib-heated channel, Hung and Lee [2] conducted transient and steady-state forced convective heat transfer studies in a vertical channel mounted with a rectangular rib, and a generalized correlation of dimensionless transient convective heat flux was proposed for the power-on transient period. Recently, laminar flow and conjugate heat transfer across three identical two-dimensional rectangular protruding blocks were theoretically analyzed using a finite difference method by Davalath and Bayazitoglu [3]. Local and average component Nusselt numbers were presented for several channel Reynolds and fluid Prandtl numbers. Furthermore, three-dimensional numerical solutions without turbulence promoters were provided by Asako and Faghri [4, 5]. Results were obtained for periodically fully-developed laminar flow and heat transfer over three-dimensional rectangular protrusions with the condition of uniform wall temperature. Supplementary computation showed that the friction factor and the Nusselt number could be predicted by two-dimensional models, depending on the geometric parameters. As with the predictions in ref. [3], the highest local Nusselt numbers along the protrusion were found near the leading edge of the face orientated parallel to the flow direction. As for the periodically fully-developed turbulent flow and heat transfer in two-dimensional ducts with rec-

† Author to whom correspondence should be addressed.

NOMENCLATURE

A_j	constants in equation (12)
a, b	constants in equation (14)
B	rib height
C_j	constants in equation (10)
C_p	coefficient of pressure drop, $\Delta P/(\frac{1}{2}\rho U_0^2)$
E_j	Nusselt number enhancement at rib j, $Nu_j/(Nu_j)_{t/H=0}$
f	Darcy friction factor, $\Delta P/[(L_c/2H)(\frac{1}{2}\rho U_0^2)]$
H	channel spacing
h	heat transfer coefficient based on inlet temperature, $q_c''/(T_w - T_0)$
j	Colburn factor, $(Nu)(Re)^{-1}(Pr)^{-1/3}$
k	thermal conductivity
L	rib length
L_c	channel length
L_r	total heating length of each rib, $2B+L$
LP	location of turbulence promoter ($LP = 1$, 2, 3, or 4), shown in Fig. 3
Nu	Nusselt number based on inlet temperature, $q_c''B/k(T_w - T_0)$
Pr	Prandtl number
ΔP	channel pressure drop between inlet and outlet
Q	heat flow rate
q''	heat flux
R	electrical resistance
Re	channel Reynolds number, $\rho U_0 H/\mu$
S	streamwise pitch of two adjacent ribs
t	turbulence promoter height
T	temperature
U_0	channel inlet velocity
V	voltage.

Greek symbols

μ	dynamic viscosity
ρ	density.

Superscript

-	average.

Subscripts

cs	steady-state convection
i	total
j	rib number
k	conduction
r	radiation
w	rib surface
x	local
0	at channel inlet.

tangular protrusions, Knight and Crawford employed the k–ε turbulence model to account for turbulence transport in the system [6, 7]. Their predictions showed good agreement with the experimental results presented by Lehmann and Wirtz [8]. In 1990, Chao [9] experimentally dealt with transient and steady-state forced convection heat transfer in a vertical insulated channel with four surface-mounted heating ribs. A generalized correlation for transient convective heat flux was also proposed and parameters such as channel spacing, steady-state convective heat flux, and channel inlet velocity affecting heat transfer performance for heating ribs were investigated extensively. In his study, it was found that the periodically fully-developed (F.D.) regime, or the so-called 'quasi-equilibrium' high-temperature regime, starts at the third rib in the range of channel Reynolds number $Re = 2182$–$29\,696$. The same conclusion for local heat transfer characteristics along the protrusion was also drawn in his study. McEntire and Webb [10] conducted a series of experiments to measure the local forced convective heat transfer characteristics of an array of protruding and flush-mounted two-dimensional discrete heat sources in a vertical channel. Air flow rates yielding effective channel Reynolds numbers Re in the range from 525 to 3937 were employed. The results of their experiments showed that the protruding heat sources yielded higher heat transfer than flush-mounted heat sources at the same channel Reynolds number. The interruption of the thermal boundary layer in the adiabatic sections between the heaters results in heat transfer enhancement. Other relevant information for discrete flush heat sources and protruding heating elements in channel flow can be found in a well organized paper survey presented by Peterson and Ortega [11].

Conceptually, the use of turbulence promoters in rib-heated channels has been corroborated to be a simple but effective means of enhancing heat transfer performance. Although turbulence promoters lead to a locally high pressure drop, they can generate a locally, suddenly accelerated flow with a high level of turbulence and thus result in a local heat transfer enhancement in the channel. In 1982, Sparrow *et al.* [12] used the naphthalene sublimation technique to measure the Sherwood number and inferred a Nusselt number for modules. They then explored the heat transfer and pressure drop for forced convection in arrays of heat generating rectangular modules deployed along one wall of a horizontal flat retangular duct, with and without barriers, and missing modules. Air was the mass transfer medium in the experiments. The implantation of a barrier in the module array was shown to be an effective enhancement device, with the greatest effect being felt in the second row downstream of the barrier while residual enhancement persisted considerably further downstream in their study. However, at the module immediately upstream of the barrier, there was a reduction in the heat transfer coefficient. Later, Sparrow *et al.* [13, 14] explored the

same problem by using multiple fence-like barriers, with the interbarrier spacing and the barrier height varied parametrically along with the Reynolds number. The main objective in ref. [13] was to determine the individual heat transfer coefficients at the top and side surfaces of the modules. Perspectives on heat transfer and pressure drop results were provided by flow visualizations performed using the oil–lampblack technique. Furthermore, the convective heat transfer response to height differences in an array of block-like electronic components was again investigated experimentally by Sparrow *et al.* [14].

The foregoing literature survey indicated that most of the existing work has only been dealing with heat transfer from single or multiple heated sources, for the most part in the periodically fully-developed regime. Moreover, although the barrier implanted on the module-sublimated wall has been studied in refs. [12–14], no information on investigating the effect of turbulence promoter, which is implanted on the opposite shrouding insulated wall, on the steady-state flow and thermal characteristics in a rib-heated channel is available in the existing literature. In order to advance our understanding on heat transfer augmentation in a vertical rib-heated channel with turbulence promoters, a series of systematic experimental investigations have been performed. The objectives of this research are to investigate the effects of channel spacing, convective heat flux, channel inlet velocity, promoter location and height on heat transfer and pressure-loss characteristics; to establish relevant correlations of Nusselt number and channel pressure drop with a wide range of system parameters studied; to explore the enhancement on heat transfer characteristics by utilizing a turbulence promoter in a rib-heated channel; and, to provide an effective cooling method for vertical PCB arrays.

THE EXPERIMENTS

Figure 1 shows the overall experimental assembly which consists of the entire apparatus and the main instruments. The measurements for the present experiments are performed in a low-turbulence open-loop wind tunnel, which is designed to be used for natural, forced, and mixed convection tests. The wind tunnel facility is in a buoyancy assisting flow condition. Detailed description of this facility has been given in ref. [15].

Test plates

The schematic of the rib-heated test plate is shown in Fig. 2. The PCB test plate is 38.0 cm wide, 28.0 cm high, and 0.4 cm thick. There are four rectangular ribs, each with a dimension of $38.0 \times 2.0 \times 1.0$ cm, mounted on the PCB surface. Each rib composes of four layers. The first layer is folded by a 0.1 cm thick stainless steel sheet. The stainless steel test surface is the primary part of the test plate. It is polished to minimize the surface roughness and emissivity, hence lessen radiative heat losses. The second layer is a 3.8×38.0 cm thermofoil heater with a thickness of 0.03 cm, epoxied on the inner surface of the first layer. The thermofoil heater, which can be applied to a voltage range of 0–140 V with 90–110 Ω resistance, is used for heating the stainless steel test surface. The emissivities of the rib surface and the PCB are estimated as 0.10 and 0.95, respectively, in the present experiments. There are 24 calibrated T-type thermocouples installed for measuring the local temperatures of each rib. The third layer is a 1.2 cm thick balsa slab, which is epoxied on the backside of the thermofoil heater to inhibit conductive heat losses from the heaters. At the backside of the balsa slab, there are four thermocouples installed to estimate the conductive heat losses. The outer layer (i.e. the fourth layer), epoxied on the backside of balsa slab and fiberglass board, is a 16.5×38 cm, 0.13 cm thick cork. Fine holes with a diameter of 0.2 cm are drilled through the balsa slab and cork to allow the passage of heater leads and thermocouples. There are a total of 154 calibrated thermocouples installed for local temperature measurements of the test plates in the experiments. In addition, a turbulence promoter is mounted on the opposite shrouding insulated wall parallel to the rib-heated test plate. The turbulence promoter, which is 38.0 cm long and 0.4 cm thick, is made of fiberglass material. A piece of L-shaped metal is attached to each lateral end of the promoter, and two metal bars with 25 screw holes are bolted to the backside of the insulated wall. Thus, the promoter can be slid along the insulated wall to the desired position, and then fastened on the insulated wall with four 1/16 in. screws. Consequently, the effect of the promoter on flow and thermal characteristics in the vertical rib-heated channel can easily be investigated in the experiments.

Apparatus and instrumentation

As previously described, the test plate has four 90–110 Ω resistive thermofoil heaters embedded in the rectangular ribs for heating, and 154 T-type calibrated thermocouples epoxied on specified locations for temperature measurements. Therefore, the local temperature distribution along the test surface including the array of ribs is accurately measured. The air temperatures at the inlet and outlet of the test channel are also measured respectively with two T-type thermocouples. The temperature difference, measured by two thermocouples at either the inlet or outlet, is consistently small.

Four d.c. power supplies (Model: GW GPD-6030D, maximum ratings: 60 V and 30 A) provide power to the heaters for making the input power changeable. A digital multimeter (Yokogawa-Model 2502A, resolution: 1 μV on 100 mV range and 1 mΩ on 100 Ω range) is utilized to calibrate the voltage of each d.c. power supply. The channel spacing between the test plate and an adiabatic shrouding plate is measured by a 150 ± 0.05 mm Mitutoyo vernier

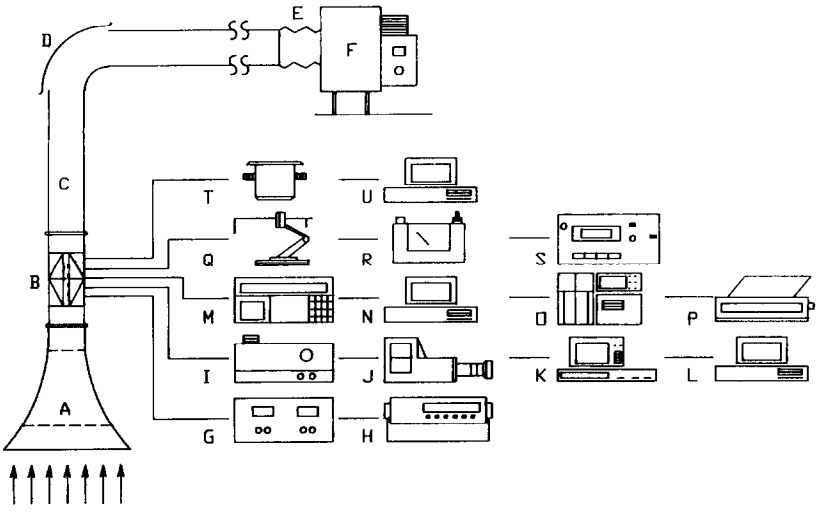

FIG. 1. Overall experimental setup.

caliper. Moreover, both the horizontal and vertical test plates are calibrated by a water level.

As for the velocity measuring system, it includes a precise hot wire anemometer (Model: V-01-AND) and a Dwyer microtector with high precision pressure measurements. The microtector delivers repeatable accuracy in measuring positive, negative, or differential pressure to ± 0.00025 in. water column over a 0.0–2.0 in. water column range. Precise calibration between the dynamic pressure head and air velocity, measured by the microtector and by the hot wire anemometer respectively, is made in the experiments.

Static pressure measurements along the opposite shrouding insulated wall are achieved using a series of micro-pressure differential transducers (Model: PR-72) connected to an IBM PC-AT computer with a data acquisition interface card (Model: Labtech DAS-16) and control software.

Data acquisition and control

The experiments are controlled and data acquired automatically with a Fluke-2280B data logging system interfaced to PC-AT based peripherals. The interface between the computer and the test plate is a 2280 Digital Acquisition and Control Unit. The unit has 160 channels of scannable thermally-compensated relays which are connected to the thermocouples. The data logging system records the air temperature at the channel inlet/outlet and the local temperature distributions of the test plates in the experiments.

Data reduction

The objective of data reduction in the experiments is to use an effective model for calculating the heat losses of the rib-heated test plate and obtaining an accurate convective heat flux, so as to get the local and average heat transfer coefficients (or Nusselt numbers) in the test channel.

The primary data-reduction program, 'PROLOG', is designed to perform data acquisition, inspection for anomalous behavior, storage, and manipulation. This program can automatically record the measured temperature data on a floppy disk. Another important data-reduction program, 'DIFC', is also developed to analyze primitive data acquired from 'PROLOG'. The fundamental concept in the 'DIFC' program for the present experiments is based on the following equation:

$$Q_c = Q_i - Q_r - Q_k - Q_t. \quad (1)$$

This energy-balance equation calculates the net convective heat flow rate, Q_c, from the test surface to the air in the test channel. The total power input to each rib is Q_i and it equals V_j^2/R_j. Here V_j represents the output voltage of each d.c. power supply and R_j

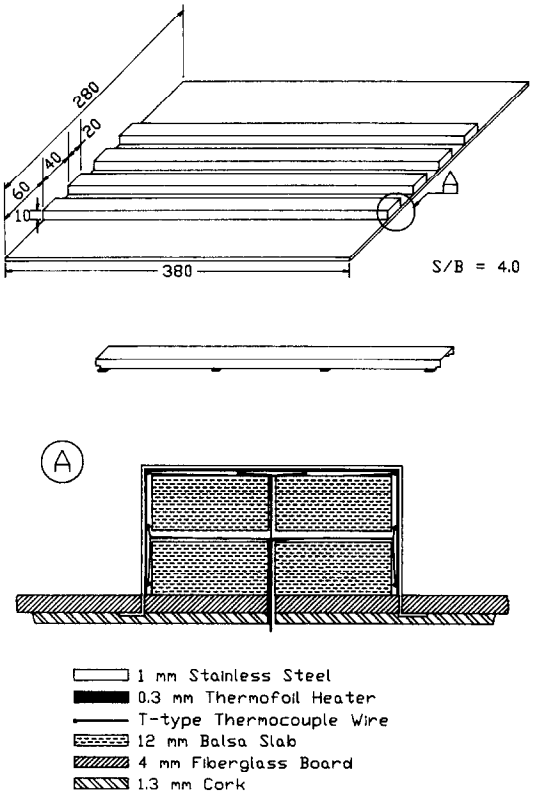

FIG. 2. Schematic of rib-heated test plate in experiments.

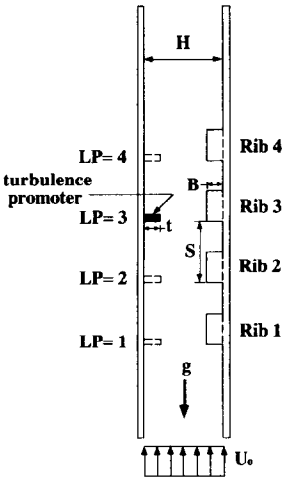

FIG. 3. Test channel investigated in experiments.

the resistance of each thermofoil heater. Q_r is the radiative heat loss from the stainless steel surface to its surroundings. It is evaluated with thermal diffuse gray-body networks. The networks establish the relationships of radiative interactions among rib surfaces, the base wall, the shrouding wall, and the ambient surroundings [16]. According to the results of radiation analysis, the maximum radiative heat loss is less than 1.1% of the total input power for all the cases considered in the present study. Q_k is the conductive heat loss to the insulated PCB and balsa slab. It is evaluated by one-dimensional (for the PCB) and two-dimensional (for the balsa slab) conduction models [16]. In the present experiments, Q_k varies from 8.0 to 11.3% for each rib of the typical cases. Q_t is the internal-energy change of the stainless steel sheet and the balsa wood during the experimental period. The method for the evaluation of internal-energy change Q_t had been introduced in refs. [16, 17].

To perform the above calculations, it should be noticed that the heat losses through the lead wires and thermocouples are so small that they are to be neglected in the experiments.

Before the experimental results of the steady-state condition are displayed, it is necessary to clarify the steady state of each experiment. Usually, the steady-state condition is considered to be achieved when Q_t approaches zero; the Q_r and Q_k reach their steady-state values, respectively; and the Q_c variation with time is less than 1.0% of the previous Q_c value in each experiment. In general, the steady-state condition can be achieved about 30 min after the power is turned on. Furthermore, to ensure the reliability of the experimental steady-state results, a group of data with a minimum absolute Q_t/Q_i value during the steady-state period are chosen as the data base for each case. After Q_i, Q_r, Q_k and Q_t are evaluated, the net convective heat flow rate from the stainless steel surface of each rib, i.e. Q_c, can be obtained. Afterwards, the local and average Nusselt numbers at the specified locations in the steady-state experiments are finally calculated.

Uncertainty analysis

Uncertainty and sensitivity analysis is used extensively in the experimental planning stage to help design the apparatus and data reduction procedures. The method used is the standard single-sample uncertainty analysis recommended by Kline and McClintock [18] and Moffat [19]. The flow chart for uncertainty analysis and data-reduction equations for the main measured quantities are shown in ref. [16]. In the experiments, temperature measurements are accurate to within $\pm 0.2^\circ C$, the uncertainty of the heat flux q_j'' is determined to be 0.25%, and those of Re and Nu for the ranges of parameters studied in the experiments are within 6.24 and 4.54%, respectively.

RESULTS AND DISCUSSION

The main emphasis of the experimental results is on forced convection heat transfer with turbulence promoter in a vertical channel mounted with four rectangular ribs. The schematic of the test channel used in the experiments is shown in Fig. 3. The discrete heating ribs are made 2.0 cm long and 1.0 cm high (i.e. $B = 1.0$ cm) and the ratio of rib pitch height S/B is designed as 4.0. Therefore, the essential parameters studied in the experiments are H/B between 2.5 and 10, q_{cs}'' ranged from 200 to 630 W m^{-2}, U_0 varied from

1.27 to 5.76 m s^{-1}, LP chosen at one of the designed locations as shown in Fig. 3 (i.e. $LP = 1$, 2, 3, or 4), and t/H ranged from 0.0 to 0.6. Sixty-six data sets with various above-mentioned parameters are presented in this research. In the study, the case with $H/B = 5.0$, $t/H = 0.2$, $LP = 3$, $U_0 \approx 3.84$ m s^{-1} and $q''_{cs,j} \approx 358$ W m^{-2} for each of the four ribs is chosen as the typical reference for comparisons.

For conventional heat transfer study in forced convection, the channel inlet temperature T_0 is usually chosen as a reference to explore heat transfer phenomena in vertical channels, especially for the study of channel-spacing effect on heat transfer characteristics. The same reference is chosen here in the present study.

The spanwise dimension of the test channel is 38.0 cm, an adequate width, to assume a two-dimensional flow for the channel spacings studied in the experiments. This assumption can be verified from the measurement of spanwise temperature distributions. The spanwise temperatures on the test surface are measured along three columns. The span between two adjacent columns is, measured in the direction normal to the streamwise air flow, 10 cm. There are 46 calibrated T-type thermocouples installed along the streamwise direction in each column. As compared with the local measured temperatures at the center column of the test section, the maximum deviations of the spanwise temperatures for the left column and the right column are less than 7.6 and 3.7%, respectively, in the range of parameters studied. This spanwise uniformity is consistent with the measured results for the 90 deg rib configuration without promoters at $Re = 12\,500$–$28\,500$, presented by Metzger *et al.* [20]. Therefore, the assumption of two-dimensional distribution may be assured during the steady-state periods, and the temperature distributions along the middle column are employed as representative of the whole test surface in the experiments.

Definition of rib heat-transfer parameters

According to the definition of Newton's law of cooling, the local convective heat transfer from each rib can be expressed as

$$q''_{cs,j} = h_{j,x}(T_{wj,x} - T_0) \tag{2}$$

where j represents the rib number. $q''_{cs,j}$ are the steady-state convective heat fluxes for the four ribs in the channel and they are kept almost the same, by means of controlling four power supplies independently, in each experimental case. For instance, the steady-state heating conditions of the four ribs for the typical case are $q''_{cs,1} = 357.32$ W m^{-2}, $q''_{cs,2} = 358.23$ W m^{-2}, $q''_{cs,3} = 358.07$ W m^{-2}, $q''_{cs,4} = 356.38$ W m^{-2}, respectively.

Thus, the local heat transfer coefficient for any one of the ribs, i.e. $h_{j,x}$ becomes

$$h_{j,x} = q''_{cs,j}/(T_{wj,x} - T_0). \tag{3}$$

From equation (3), the average heat transfer coefficients of the jth rib based on T_0 can be expressed as

$$\bar{h}_j = \frac{1}{L_r}\int_0^{L_r} h_{j,x}\,dx = \frac{q''_{cs,j}}{L_r}\int_0^{L_r}\frac{1}{(T_{wj,x} - T_0)}\,dx \tag{4}$$

where L_r represents the total heating length of each rib, i.e. $L_r = 2B + L$.

The integration of equation (4) is approximated by summing up all products of the reciprocal of local temperature difference, i.e. $1/(T_{wj,x} - T_0)$, and the corresponding length of segment Δx. Thus

$$\bar{h}_j \approx \frac{q''_{cs,j}}{L_r}\Sigma\frac{1}{(T_{wj,x} - T_0)}\Delta x. \tag{5}$$

Thus, the average Nusselt number base on the rib height B ($B = 1$ cm in the present experiments) for each rib is

$$Nu_j = \bar{h}_j B/k. \tag{6}$$

Consequently, the overall average Nusselt number $\overline{Nu}$ in the channel can be evaluated as the average value of Nusselt numbers of the four heating ribs.

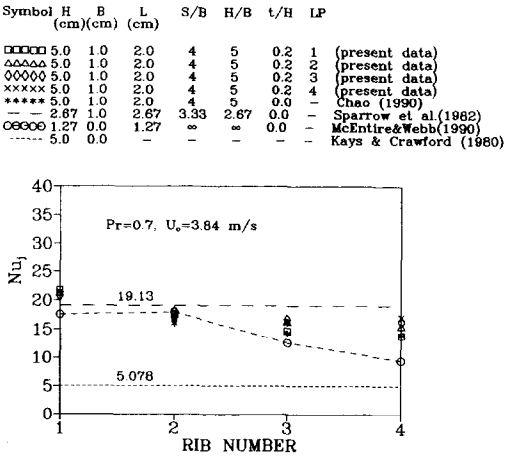

FIG. 4. Nu_j distributions for typical case.

Average heat transfer characteristics of the ribs

Figure 4 shows the distributions of average rib Nusselt number, based on channel inlet temperature T_0, for the cases of $S/B = 4$, $H/B = 5$, $t/H = 0.2$ and $U_0 = 3.84$ m s^{-1} with various promoter locations (i.e. $LP = 1$, 2, 3, or 4). From the results of the typical case shown in the figure, it is evidenced that the heat transfer performance of rib 1 is better than that of rib 3 or rib 4 for about 26% in the steady-state condition. However, as seen in ref. [9], where the test channel was the same as the one used in the present experiments except without turbulence promoters, the heat transfer performance of rib 1 was better than that of rib 3 or rib 4 for about 53% in the steady-state

condition. Moreover, during the steady-state period in ref. [9], it was also manifested that the heat transfer characteristics for ribs 3 and 4 had the same trend, and the relative deviation on heat transfer characteristics between them could be negligible if the experimental uncertainties were taken into consideration. According to the above-mentioned experimental results in ref. [9], it may be assumed, similarly, that the so-called 'fully-developed' or 'quasi-equilibrium' high-temperature regime starts at the third rib in the range of channel inlet velocity studied in the present forced-convection experiments. This result is closely consistent with that investigated by Sparrow *et al.* [12]. They concluded that the fully-developed heat transfer coefficients were encountered starting with the fifth and all subsequent rows. Although the fully-developed heat transfer regime in ref. [12] slightly lagged behind that of the present experiments, the trend can be reasonably seen by observing that the channel entrance effect on three-dimensional modules used in ref. [12] is much stronger than that of the two-dimensional ribs in the present study. The experimental results obviously support the observation that the use of turbulence promoter can improve the heat transfer performance in the 'quasi-equilibrium' region effectively. In addition, it is worth noting that the turbulence promoter installed on the opposite shrouding wall enhances not only the heat transfer performance of its downstream ribs but also that of its upstream ribs. As compared with the experimental results presented in refs. [12, 13], the current study obviously shows that the present promoter installation on the opposite shrouding wall is better than that on the rib-heated wall, for the consideration of heat transfer enhancement. In Fig. 4, three relevant results in the existing literature are also shown for comparisons. The first one is the Nusselt number for fully developed turbulent flow between parallel smooth planes with one side isoflux heated and the other insulated [21]. The second one is calculated from the equations for flush-mounted heater configurations proposed by McEntire and Webb [10]

$$Nu_j = \begin{cases} 0.772\,Re^{0.39}, & j=1 \\ 0.574\,Re^{0.43}, & j=2 \\ 0.372\,Re^{0.44}, & j=3 \\ 0.576\,Re^{0.35}, & j=4 \end{cases} \quad (7)$$

where the above equations are valid for the cases of $H = 1.27$ cm and $L = 1.27$ cm with the range of $Re = 525$–3937.

The third one is the fully-developed Nusselt number for three-dimensional modules at $U_0 = 3.84$ m s^{-1}, which is evaluated from the following equation [12]:

$$Nu = 0.0351\,Re^{0.72}, \quad Re = 2000\text{–}7000 \quad (8)$$

where equation (8) is valid only for the cases with $S/B = 3.33$, $H/B = 2.67$, $B = 1.0$ cm and $L = 2.67$ cm.

The comparisons between the present data and

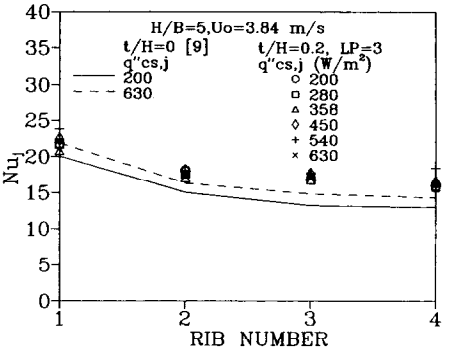

(a) effect of convective heat flux

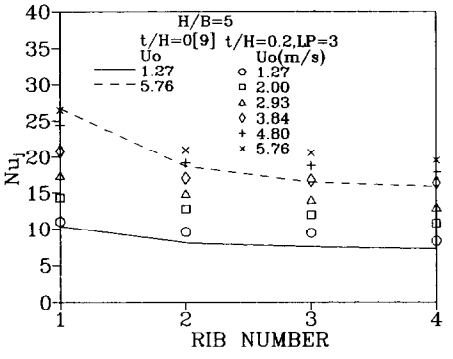

(b) effect of channel inlet velocity

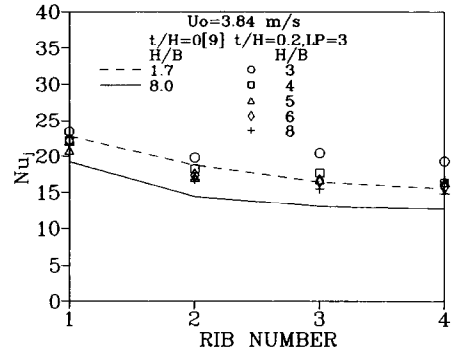

(c) effect of channel spacing

FIG. 5. Effects of relevant parameters on rib heat transfer characteristics.

either of the first two relevant results show the effect of rib obstructions on heat transfer enhancement; while the comparisons of the present data with the third relevant results display the geometric effect on heat transfer performance.

As shown in Figs. 5(a)–(c), the effects of convective heat flux, channel inlet velocity and channel spacing on rib heat transfer characteristics are presented. In Fig. 5(a), the convective heat flux has no significant effects on the average rib Nusselt number in the present forced-convection cases. This manifests that the heat transfer performance in the present experiments is not affected by buoyancy, and the heat transfer mechanism may be considered as purely forced con-

vection. Moreover, the results for the cases without turbulence promoters in ref. [9] are also plotted in the figure for comparisons. From the figure, the promoter ($LP = 3$) not only increases the Nusselt number of the ribs in its downstream, but also increases the Nusselt number of ribs in its upstream.

Figure 5(b) shows the effect of channel inlet velocity on rib heat transfer characteristics. For the case of $H/B = 5$, $t/H = 0.2$, $LP = 3$ and $q''_{cs,j} = 358$ W m^{-2} with various inlet velocities, it is found that the average Nusselt number increases with increasing channel inlet velocity U_0. This observation agrees with what is physically expected in forced convection. In addition, the promoter also has the same trend to enhance its downstream and upstream average Nusselt numbers as discussed in Fig. 5(a).

To investigate the effect of channel spacing on rib heat transfer performance, Fig. 5(c) displays the results for the case of $LP = 3$, $q''_{cs,j} = 358$ W m^{-2} and $U_0 = 3.84$ m s^{-1} with various channel spacings. The figure indicates that the average Nusselt number will increase when the H/B ratio decreases. This tendency may be properly explained by the magnitude of flow acceleration that occurs in the effective contraction passage of the channel for various H/B ratios. As we know, when the channel inlet velocity is fixed, say $U_0 = 3.84$ m s^{-1}, the cross-sectional area of the free flow passage formed by the obstructive ribs and the promoter decreases with decreasing channel spacing; therefore, the effective flow velocity will increase and the heat transfer performance will consequently be improved with the decreased channel spacing. In other words, we may conclude that the smaller the channel spacing is, the larger the average Nusselt number Nu_j for each rib becomes. The turbulence promoter also has the same effects in increasing its downstream and upstream average Nusselt number as found in Figs. 5(a) and (b).

Prior to exploring the effect of turbulence promoter location on rib heat transfer performance, two types of promoter installation, which will be compared with each other in the following paragraphs, should be described here. Figures 6(a) and (b) depict respectively the present installation method along with the ranges of relevant parameters studied and those proposed by Sparrow *et al.* [12].

The results presented in Fig. 4 verify that the turbulence promoter location affects the heat transfer performances of its downstream and upstream heating ribs. The Nusselt number enhancement observed at the rib immediately downstream of the promoter is greater than that at other locations. For the typical case shown in Fig. 7, with increasing upstream or downstream distance from the promoter, the extent of the heat transfer enhancement of the heating rib gradually drops off. Therefore, according to the experimental data, the Nusselt number enhancement for the rib downstream or upstream of the promoter (i.e. $Nu_j/(Nu_j)_{t/H=0}$) can be normalized by that for the rib immediately downstream of the promoter (i.e. $Nu_{j-lp}/(Nu_{j-lp})_{t/H=0}$). Then, the relationship between this normalized Nusselt number enhancement at rib j and the corresponding relative location ($j-LP$) in the present study may be expressed in an exponential distribution form:

$$\frac{E_j}{E_{j=lp}} = e^{-0.02(j-lp)^2} \tag{9}$$

where E_j is defined as $Nu_j/(Nu_j)_{t/H=0}$, and $E_j/E_{j=lp}$ represents the ratio of the average Nusselt number enhancement at any rib j to that at the rib immediately downstream of the promoter $j = LP$ (e.g. at rib 3 for $LP = 3$).

The average deviation of the predictions using the above equation from the experimental data is 4.4%.

Furthermore, the effect of the implanted barrier on heat transfer enhancement, which was studied in ref. [12], is also interpreted and shown in Fig. 7. Their results showed that the barrier effectively fulfilled its function as a heat transfer enhancement device, with the greatest enhancements occurring in the second row downstream of the barrier. In the ranges of their experimental parameters studied (see Fig. 6(b)), they found that the reattachment of the flow, which lifted off due to the presence of the barrier, took place in the second row, making the heat transfer coefficients at the second-row modules greater than those in the first row. Another noteworthy feature of their results was that there was a reduction in the heat transfer coefficient at the modules upstream of the barrier. To overcome this heat transfer defect, the turbulence promoter installed on the opposite shrouding insulated wall in the present study reveals its major advantage in preventing the occurrence of local hot spots from the heating process. Additionally, the rib heat transfer performances in the channel are all enhanced, with the greatest heat transfer enhancement occurring at the rib immediately downstream of the promoter. The main reason is that the forced flow abruptly lifts off due to the presence of the promoter mounted on the shrouding insulated wall, and transversely accelerates its velocity nearby the rib immediately downstream of the promoter.

As for the effect of the ratio of promoter height to channel spacing t/H on average rib Nusselt number Nu_j and overall average $\overline{Nu}$, the experimental results are shown in Figs. 8(a) and (b). They manifest a significant effect of t/H ratio on average Nusselt number Nu (or overall average $\overline{Nu}$) distribution. The Nu (or $\overline{Nu}$) value increases with increasing t/H ratio. In general, the relationship between Nu (or $\overline{Nu}$) and t/H in the present study can be expressed as

$$\frac{(Nu_j)_{t/H}}{(Nu_j)_{t/H=0}} = 1 + C_j\left(\frac{t}{H}\right), \quad j = 1, 2, 3, \text{or } 4 \tag{10}$$

where the constants $C_1 = 0.0298$, $C_2 = 0.475$, $C_3 = 1.530$, and $C_4 = 1.184$

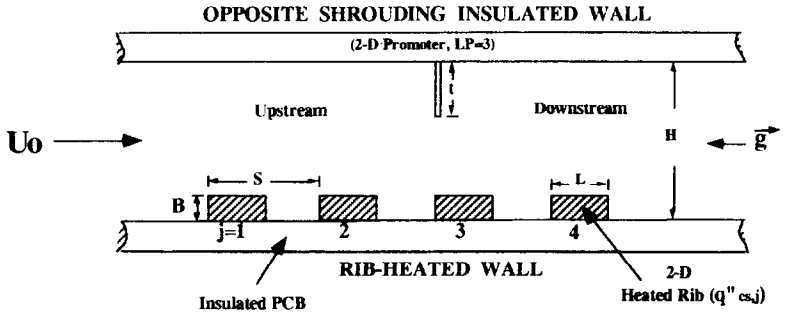

Parameters Studied

S/B=4.0, H/B=2.5-10.0, B/L=0.5, t/H=0.0-0.6, t/B=0.0-4.5, LP=1-4, B=1.0cm
Pr=0.7 (AIR), q" cs,j=200-630W/m , Uo=1.27-5.76m/s, Re=3887-29524

(a) turbulence - promoter installation in the present study

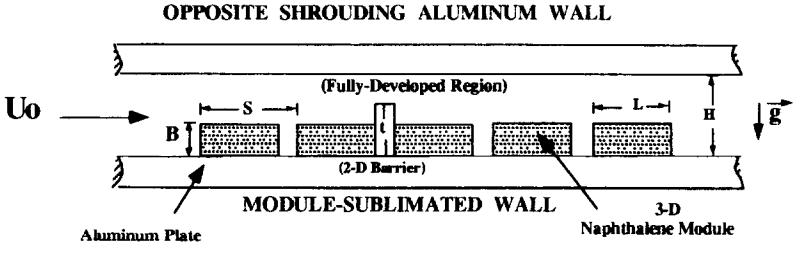

Parameters Studied

S/B=3.33, H/B=2.67, B/L=0.375, t/H=0.5-0.75, B=1.0cm
Pr=0.7 (AIR), Re=2000-7000

(b) barrier installation in (Sparrow et al., 1982, 1983)

FIG. 6. Comparison of promoter installation method in present study with that in refs. [12, 13].

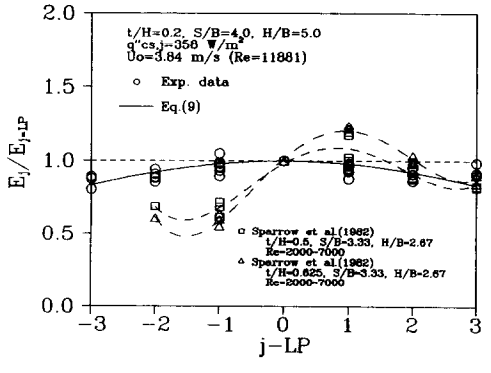

FIG. 7. Distributions of dimensionless Nu_j enhancement for various relative rib locations.

$$\frac{(\overline{Nu})_{t/H}}{(\overline{Nu})_{t/H=0}} = 1+0.692\left(\frac{t}{H}\right). \tag{11}$$

The average deviations of the predictions using the above equations from the experimental data are 3.5% (rib 1), 3.3% (rib 2), 4.5% (rib 3), 3.2% (rib 4) and 2.9% (average), respectively.

Furthermore, from the above-presented results, it is reconfirmed that the heat transfer performances for the heating ribs in the channel are all enhanced; and the greatest Nusselt number can be found at the rib immediately downstream of the promoter. With increasing upstream or downstream distance of the heating rib from the promoter, the extent of the heat transfer enhancement gradually drops off.

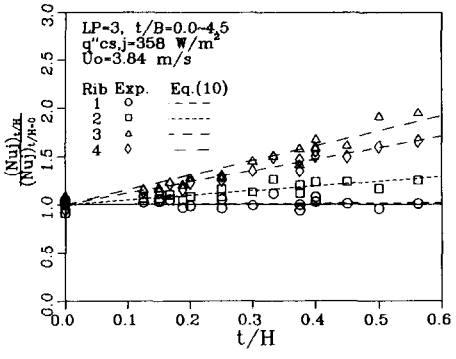

(a) t/H effect on $Nu_j/(Nu_j)_{t/H=0}$

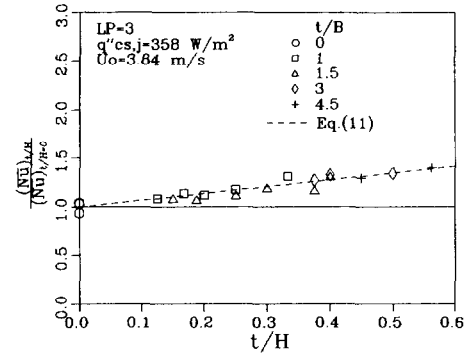

(b) t/H effect on $\overline{Nu}/\overline{(Nu)}_{t/H=0}$

FIG. 8. $Nu/(Nu)_{t/H=0}$ distributions in experiments.

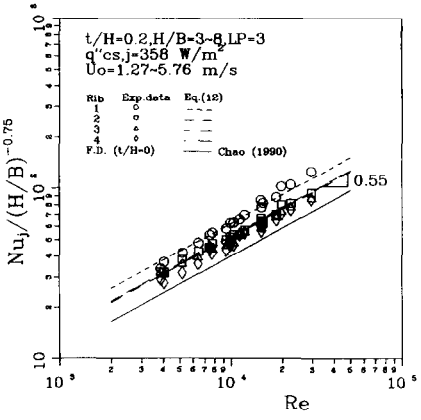

(a) relationship among Nu_j, H/B and Re

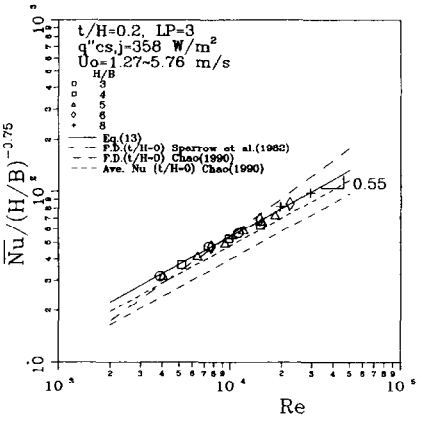

(b) relationship among $\overline{Nu}$, H/B and Re

FIG. 9. Relationship among Nu, H/B and t/H for heating ribs.

Figures 9(a) and (b) show the relationships among the average rib Nusselt numbers Nu_j (or overall average $\overline{Nu}$), ratio of channel spacing to rib height H/B, and Reynolds number Re for heating ribs. All the properties used for the Nu and Re calculations are based on the channel inlet temperature. From these figures, it is found that Nu (or $\overline{Nu}$) depends on Re as a 0.55 power for cases with a specific H/B ratio. The Reynolds number dependence of a 0.55 power is consistent with the 0.53 power dependence presented by McEntire and Webb [10] for the cases with protruding two-dimensional discrete heat sources, although their experimental cases were all in the laminar or transition range. The 0.55 power proposed in the present study is substantially higher than the 0.4 dependence observed for the flush-mounted heater configuration [10]. This is also somewhat different from a 0.75 power for the large ribbed roughness experiments with $S/B = 4$ and $H/B = 4.6$, where S is the streamwise pitch between two adjacent ribs (measured centerline to centerline), presented by Arvizu and Moffat [22].

In addition, from the experimental data it is also evident that Nu is inversely proportional to the H/B ratio with a 0.75 power dependence. Therefore, based on the present experimental data, the relationships between $Nu_j/(H/B)^{-0.75}$ (or $\overline{Nu}/(H/B)^{-0.75}$) and Reynolds number Re can be correlated in the following forms:

$$Nu_j/(H/B)^{-0.75} = A_j\, Re^{0.55}, \quad j = 1, 2, 3, \text{ or } 4 \qquad (12)$$

where $A_1 = 0.394$, $A_2 = 0.332$, $A_3 = 0.329$ and $A_4 = 0.325$; and

$$\overline{Nu}/(H/B)^{-0.75} = 0.344\, Re^{0.55}. \qquad (13)$$

In Figs. 9(a) and (b), the fully-developed Nu_j correlations for the cases without mounting promoters or barrier, i.e. $t/H = 0$, in refs. [9, 12] are also shown for comparisons. In ref. [9], the fully-developed A_j in equation (12) and the mean value in equation (13) are 0.252 and 0.302, respectively. Figure 9(b), which presents the correlation proposed by Sparrow *et al.* [12], i.e. equation (8), manifests that the Nusselt numbers are more strongly dependent on Reynolds number in the ranges of their experimental parameters studied (see Fig. 6(b)).

Finally, if the parameters Re, H/B, t/H and relative downstream (or upstream) rib location $(j-LP)$, which all affect the heat transfer performance, are simultaneously taken into consideration, five empirical correlations related to Nu (or $\overline{Nu}$), Re, H/B, t/H and $(j-LP)$ can be obtained by using a curve-fitting

method. These new empirical correlations are proposed as

$$Nu_j = a\,Re^{0.55}(H/B)^{-0.75}[1+b\,e^{-0.02(j-lp)^2}(t/H)] \tag{14}$$

where

$$j=\begin{cases}1: a=0.392, & b=0.0323\\ 2: a=0.303, & b=0.485\\ 3: a=0.263, & b=1.255\\ 4: a=0.252, & b=1.448\end{cases}$$

and

$$\overline{Nu} = 0.302\,Re^{0.55}(H/B)^{-0.75}[1+0.692(t/H)] \tag{15}$$

where Nu and Re are based on the rib height B and channel spacing H, respectively. The comparisons between the experimental data and the predictions from equations (14) and (15) are made and shown in Fig. 10. The data points for comparisons are 330. The range of the parameters H/B, t/H, $q''_{cs,j}$, U_0 and LP where equations (14) and (15) are applicable is also given in the figure. The average deviations of the predictions by equations (14) and (15) compared with the present experimental data are 4.9, 4.3, 5.5, 7.7 and 5.3% for Nu_1, Nu_2, Nu_3, Nu_4 and $\overline{Nu}$, respectively.

Effect of turbulence promoter on overall channel pressure drop

In general, two important characteristics, i.e. heat transfer performance and pressure drop, should be investigated in experiments of heat transfer and fluid dynamics. From the experimental results presented in the previous subsections, it is clearly shown that the installation of turbulence promoter in the test channel can improve rib/overall heat transfer performance and prevent the occurrence of hot spots from the heating process in the fully-developed regime of the channel. However, the promoter installation also obstructs the flow and increases the pressure losses.

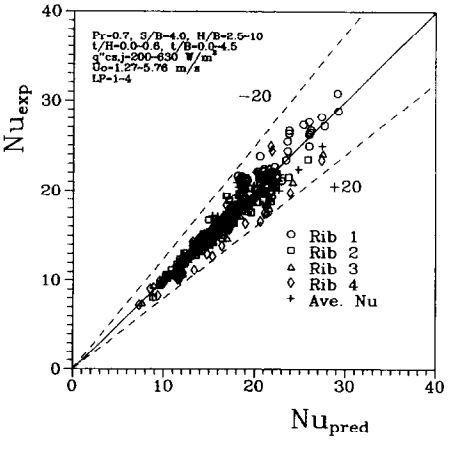

FIG. 10. Comparisons of experimental data with predictions from equation (14) or (15).

This means more power is needed to maintain the same flow rate as in a channel without turbulence promoters. Thus, the following will discuss the channel pressure loss from the frictional aspect.

As we know, the definition of the coefficient of pressure losses in the channel can be expressed in the following form:

$$C_p = \frac{\Delta P}{1/2\rho U_0^2} \tag{16}$$

where ΔP represents the static pressure drop between the inlet and outlet of the channel.

As shown in Fig. 11, the ratio of C_p for cases with a promoter to that in the corresponding cases without a promoter, i.e. $C_p/(C_p)_{t/H=0}$, is significantly affected by the ratio of promoter height to channel spacing t/H; while not significantly affected by any one of the following parameters: H/B, t/B, $q''_{cs,j}$, U_0, and LP. In refs. [12, 22], it was similarly observed that the dimensionless pressure drop is a weak function of Reynolds number for a ribbed channel without a promoter or with a barrier. This finding indicates that the pressure losses are primarily due to inertial effects. In the present study, for parameter ranges of $H/B = 2.5$–10, $t/B = 0.0$–4.5, $q''_{cs,j} = 200$–$630\ \mathrm{W\,m^{-2}}$, $U_0 = 1.27$–$5.76\ \mathrm{m\,s^{-1}}$ (or $Re = 3887$–$29\,524$) and $LP = 1$–4, the $C_p/(C_p)_{t/H=0}$ distribution can be proposed as a function of t/H only and expressed in the following curve-fitted form

$$C_p/(C_p)_{t/H=0} = 1+86.58(t/H)^2. \tag{17}$$

The average deviation of the predictions using the above equation from the experimental data is 19.1%.

From equations (11) and (17), it is evident that higher promoters are more advantageous for heat transfer enhancement; however, there is a severe penalty in pressure drop. This conclusion is qualitatively consistent with the results presented in ref. [12]. Taking into consideration a four-row ribbed channel with a promoter or a barrier, a quantitative comparison between the present study and that by Sparrow *et al.* [12] is also shown in Fig. 11. At any specific t/H value, say 0.5, the pressure drop in the present study is larger than that in ref. [12]. The main reason is that, in the

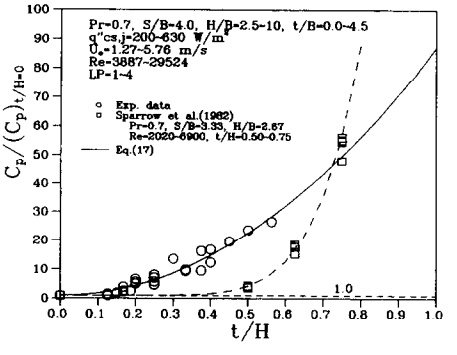

FIG. 11. $C_p/(C_p)_{t/H=0}$ distributions for various t/H ratios.

present study, the ratio of the effective flow cross-sectional area at the promoter location to the frontal channel area is much smaller, which causes a larger pressure drop [23]. Furthermore, from the trend of the pressure-drop distributions for cases of $t/H < 0.6$ shown in the figure, the higher the promoter or barrier is, the smaller the difference is between the pressure drops in the present study and in ref. [12].

Similar to the concept of maximum value of AEHT (Amount of Enhanced Heat Transfer) introduced in ref. [24], the Colburn factor for heat transfer j and Darcy friction factor for channel pressure drop f can be defined, respectively, as

$$j = (Nu)(Re)^{-1}(Pr)^{-1/3} \tag{18}$$

where Pr is the Prandtl number of fluid and

$$f = \Delta P/[(L_c/2H)(\rho V_0^2/2)] \tag{19}$$

where L_c represents the channel length and $2H$, the hydraulic diameter for a two-dimensional parallel channel.

Under a specified geometric rib-heated channel with the same experimental conditions, the j/f ratio, the so-called AEHT, is proportional to the Nu/C_p ratio. Therefore, the j/f ratios between the cases with and without a promoter can be expressed as

$$\frac{j/f}{(j/f)_{t/H=0}} = \frac{Nu/C_p}{(Nu/C_p)_{t/H=0}} \tag{20}$$

i.e. the equation can be obtained from equation (11) divided by equation (17).

Figure 12 depicts the relationship between j/f and t/H. The average deviation of the predictions by equation (20) compared to the present experimental data is 18.2%. The experimental results manifest that if both the standpoints of heat transfer enhancement and pressure drop are simultaneously considered (for example, in aeronautic applications), the use of a promoter may not be valuable for higher t/H cases. The results in ref. [12] had introduced a similar trend. However, if more emphasis is put on enhancing heat transfer performance and preventing the occurrence of hot spots from the heating process in the rib-heated channel, the present installation of a turbulence promoter is better than that studied in ref. [12]. In other words, in the present study, heat transfer enhancements are achieved for all the ribs both upstream and downstream of the promoter, not merely on the modules downstream of the barrier as in ref. [12].

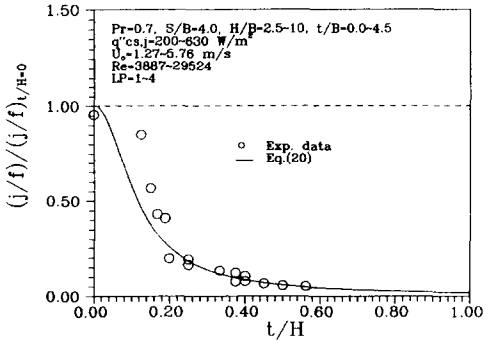

FIG. 12. $(j/f)/(j/f)_{t/H=0}$ distributions for various t/H ratios.

CONCLUDING REMARKS

Experimental investigation of forced convection with a turbulence promoter in a vertical rib-heated channel has been systematically performed in this research. The main conclusions emerging from the results and discussion may be summarized as follows:

(1) The use of a turbulence promoter can effectively improve the heat transfer characteristics and avoid the occurrence of hot spots in the 'quasi-equilibrium' high-temperature regime. In addition, it enhances not only the heat transfer performance of its downstream ribs, but also that of its upstream ribs.

(2) The heat transfer performance for each rib will increase when the H/B ratio decreases. This tendency can be reasonably explained by the increase of flow acceleration in the effective contraction passage of the channel with decreasing H/B ratio.

(3) The effect of convective heat flux on rib heat transfer performance is insignificant; on the other hand, the effect of channel inlet velocity is significant, the heat transfer performance increases with increasing channel inlet velocity. This observation agrees to what is physically expected in forced convection.

(4) The greatest Nusselt number occurs at the rib immediately downstream of the promoter. With increasing upstream or downstream distance of the heating rib from the promoter, the extent of the heat enhancement gradually drops off.

(5) The t/H effect is, compared with the effect of promoter location, more significant on heat transfer performance. The Nusselt number will increase when the t/H ratio increases.

(6) Nu depends on Re as a 0.55 power for cases with a specified H/B ratio. In addition, Nu is inversely proportional to the H/B ratio with a 0.75 power dependence.

(7) Empirical correlations related to Nu, Re, H/B, t/H and $(j-LP)$ are proposed, and the average relative deviation between the experimental data and the predictions is 5.3%.

(8) As compared with the effect of promoter location, the t/H effect on overall channel pressure drop is more significant. The coefficient of pressure losses C_p increases with increasing t/H ratio.

(9) If both the standpoints of heat transfer enhancement and pressure drop are simultaneously considered, the use of promoter may not be valuable for higher t/H cases. If more emphasis is put on enhancing heat transfer performance and preventing the occurrence of hot spots from the heating process in the rib-heated channel, the present installation of a

turbulence promoter is better than those studied in existing literature.

REFERENCES

1. A. Bar-Cohen and W. M. Rohsenow, Thermally optimum spacing of vertical, natural convection cooled, parallel plates, *ASME J. Heat Transfer* **106,** 116–123 (1984).
2. Y. H. Hung and D. Y. Lee, Transient forced-convective heat transfer in a vertical channel mounted with a rectangular rib. In *Transport Phenomena in Thermal Control* (Edited by G. J. Hwang), pp. 115–126. Hemisphere, New York (1989).
3. J. Davalath and Y. Bayazitoglu, Forced convection cooling across rectangular blocks, *ASME J. Heat Transfer* **109,** 321–328 (1987).
4. Y. Asako and M. Faghri, Three-dimensional heat transfer and fluid flow analysis of arrays of square blocks encountered in electronic equipment, *Numer. Heat Transfer* **13,** 481–498 (1988).
5. Y. Asako and M. Faghri, Three-dimensional heat transfer analysis of arrays of heated square blocks, *Int. J. Heat Mass Transfer* **32,** 395–405 (1989).
6. R. W. Knight and M. E. Crawford, Simulation of convective heat transfer in pipes and channels with periodically varying cross-sectional area. In *Numerical Methods in Thermal Problems*, Vol. 5, pp. 512–523. Pineridge Press, Swansea (1987).
7. R. W. Knight and M. E. Crawford, Numerical prediction of turbulent flow and heat transfer in channels with periodically varying cross sectional area, *Proc. 1988 Natn. Heat Transfer Conf.*, Vol. 1, pp. 669–676. ASME, New York (1988).
8. G. L. Lehmann and R. A. Wirtz, The effect of variations in stream-wise spacing and length on convection from surface mounted rectangular components. In *Heat Transfer in Electronic Equipment*, pp. 39–47. ASME, New York (1985).
9. S. D. Chao, An experimental study on forced convection heat transfer characteristics in vertical adiabatic channels with surface-mounted heating ribs, Master's Thesis, Department of Power Mechanical Engineering, National Tsing Hua University, Taiwan, R.O.C. (June 1990).
10. A. B. McEntire and B. W. Webb, Local forced convective heat transfer from protruding and flush-mounted two-dimensional discrete heat sources, *Int. J. Heat Mass Transfer* **33,** 1521–1533 (1990).
11. G. P. Peterson and A. Ortega, Thermal control of electronic equipment and devices. In *Advances in Heat Transfer*, Vol. 20, pp. 181–314. Academic Press, New York (1990).
12. E. M. Sparrow, J. E. Niethammer and A. Chaboki, Heat transfer and pressure drop characteristics of arrays of rectangular modules encountered in electronic equipment, *Int. J. Heat Mass Transfer* **25,** 961–973 (1982).
13. E. M. Sparrow, S. B. Vemuri and D. S. Kadle, Enhanced and local heat transfer, pressure drop, and flow visualization for arrays of block-like electronic components, *Int. J. Heat Mass Transfer* **26,** 689–699 (1983).
14. E. M. Sparrow, A. A. Yanezmoreno and D. R. Otis, Jr., Convective heat transfer response to height differences in an array of block-like electronic components, *Int. J. Heat Mass Transfer* **27,** 469–473 (1984).
15. Y. H. Hung and W. M. Shiau, Local steady-state natural convection heat transfer in vertical parallel plates with a two-dimensional rectangular rib, *Int. J. Heat Mass Transfer* **31,** 1279–1288 (1988).
16. N. T. Chang, An experimental study on heat transfer characteristics of natural convection in vertical channels with surface-mounted ribs, Master's Thesis, Department of Power Mechanical Engineering, National Tsing Hua University, Taiwan, R.O.C. (June 1989).
17. Y. H. Hung and W. M. Shiau, An effective model for measuring transient natural convective heat flux in vertical parallel plates with a rectangular rib, *Int. J. Heat Mass Transfer* **32,** 863–871 (1989).
18. S. J. Kline and F. A. McClintock, Describing uncertainties in single-sample experiments, *Mech. Engng* 3–8 (January 1953).
19. R. J. Moffat, Describing the uncertainties in experimental results, *Expl Thermal Fluid Sci.* **1,** 3–17 (1988).
20. D. E. Metzger, C. S. Fan and Y. Yu, Effects of rib angle and orientation on local heat transfer in square channels with angled roughness ribs. In *Compact Heat Exchangers*, pp. 156–158, Hemisphere, New York (1990).
21. W. M. Kays and M. E. Crawford, *Convective Heat and Mass Transfer* (2nd Edn). McGraw-Hill, New York (1980).
22. D. E. Arvizu and R. J. Moffat, Experimental heat transfer from an array of heated cubical elements on an adiabatic channel wall, Rept. No. HMT-33, Thermosciences Div., Dept. of Mech. Engng, Stanford University (1981).
23. W. D. Baines and E. G. Peterson, An investigation of flow through screens, *Trans. ASME* **73**(V), 467–480 (1951).
24. T. Kishimoto, E. Sasaki and K. Moriya, Gas cooling enhancement technology for integrated circuit chips, *IEEE Trans. Components, Hybrids, Mfg Technol.* **CHMT-7,** 286–293 (1984).

UNE DISPOSITION EFFICACE DE PROMOTEURS DE TURBULENCE POUR L'ACCROISSEMENT DE TRANSFERT THERMIQUE DANS UN CANAL VERTICAL CHAUFFE ET RAINURE

Résumé—On étudie en détail l'effet de paramètre comme la largeur du canal, le flux thermique, la vitesse d'entrée, la disposition du promoteur de turbulence et la hauteur sur les performances de transfert de chaleur et la perte de pression dans un canal vertical rainuré et chauffé. De plus les nombres de Nusselt par rainure et global et le coefficient de perte de pression C_p sont corrélés et présentés en fonction des paramètres sans dimension. Les résultats expérimentaux montrent que l'installation du promoteur de turbulence sur la paroi isolée opposée peut effectivement accroître les performances du transfert thermique des rainures dans le canal et supprimer les poches chaudes qui peuvent exister dans le régime en quasi-équilibre à haute température. Considérant à la fois les aspects thermiques et dynamiques, Nu et C_p augmentent ensemble quand le rapport t/H de la hauteur du promoteur à la largeur du canal croît. Cette tendance est cohérente avec les niveaux accrus de la perturbation de l'écoulement et du mélange par turbulence créés par les rainures et le promoteur de turbulence.

EINE WIRKSAME ANORDNUNG VON TURBULENZERZEUGERN ZUR VERBESSERUNG DER WÄRMEÜBERTRAGUNG IN EINEM SENKRECHTEN, DURCH RIPPEN BEHEIZTEN KANAL

Zusammenfassung—Der Wärmeübergang und der Druckabfall in einem senkrechten durch Rippen beheizten Kanal wurde in der vorliegenden Parameterstudie eingehend untersucht, wobei die Kanalweite, die konvektive Wärmestromdichte, die Geschwindigkeit am Eintritt in den Kanal sowie Ort und Höhe der Turbulenzerzeuger systematisch variiert wurden. Zusätzlich werden die Nusselt-Zahl für den ganzen Kanal und der Koeffizient für den Druckabfall C_p korreliert und abhängig von den wesentlichen Einflußparametern dargestellt. Die Versuchsergebnisse zeigen, daß durch Turbulenzerzeuger an der gegenüberliegenden isolierten Wand des senkrechten durch Rippen beheizten Kanals der Wärmeübergang an dieser Berippung wirksam verbessert werden kann. Außerdem werden Heißstellen vermieden, die im Hochtemperaturbereich unter Quasi-Gleichgewichtsbedingungen auftreten können. Betrachtet man gleichzeitig die Wärme- und die Impulsübertagung, so nehmen Nu und C_p mit wachsendem Verhältnis aus Höhe des Turbulenzerzeugers und Kanalweite (t/H) zu. Diese Tendenz stimmt mit der verstärkten Störung der Strömung oder mit der turbulenten Mischung überein, welche durch die hervorstehenden Rippen und die eingebauten Turbulenzerzeuger hervorgerufen werden.

ЭФФЕКТИВНОЕ РАСПОЛОЖЕНИЕ ТУРБУЛИЗАТОРОВ С ЦЕЛЬЮ ИНТЕНСИФИКАЦИИ ТЕПЛОПЕРЕНОСА В НАГРЕВАЕМОМ ВЕРТИКАЛЬНОМ ОРЕБРЕННОМ КАНАЛЕ

Аннотация—Проводится детальное исследование влияния таких параметров, как расстояние между стенками канала, конвективный тепловой поток, скорость на входе в ганал, а также расположение и высоты турбулизаторов на характеристики теплопереноса и сопротивление в нагреваемом вертикальном оребренном канале. Установлено соотношение между числами Нуссельта для оребренной и всей поверхности канала и коэффициентом сопротивления в канале C_p, которые представлены через соответствующие исследуемые безразмерные параметры. Экспериментальные данные показывают, что установка турбулизатора на противоположной экранирующей изолированной стенке в рассматриваемом канале может эффективно повысить все характеристики переноса тепла от ребер и предотвратить появление сильно нагретых участков, характерных для псевдоравновесного высокотемпературного режима. В случае одновременного учета тепловых и динамических характеристик значения Nu и C_p возрастают с увеличением отношения высоты турбулизатора к расстоянию между стенками канала t/H. Эта тенденция наблюдается одновременно с увеличением степени возмущения потока или турбулентного смешения, вызванного выступающими ребрами и установленным турбулизатором.